Received: 26 April 2021 | Revised: 7 June 2021 | Accepted: 8 June 2021

DOI: 10.1111/jon.12903

JOURNAL OF NEUROIMAGING
THE OFFICIAL JOURNAL OF THE AMERICAN SOCIETY OF NEUROIMAGING
WILEY

CLINICAL INVESTIGATIVE STUDY

Glioblastoma radiomics to predict survival: Diffusion characteristics of surrounding nonenhancing tissue to select patients for extensive resection

Luca Pasquini[1,2,#] | Alberto Di Napoli[2,3,#] | Antonio Napolitano[4] | Martina Lucignani[4] | Francesco Dellepiane[2] | Antonello Vidiri[5] | Veronica Villani[6] | Andrea Romano[2] | Alessandro Bozzao[2]

[1] Neuroradiology Service, Department of Radiology, Memorial Sloan Kettering Cancer Center, New York, USA

[2] Neuroradiology Unit, NESMOS Department, Sant'Andrea Hospital, La Sapienza University, Rome, Italy

[3] Radiology Department, Castelli Romani Hospital, Rome, Italy

[4] Medical Physics Department, Bambino Gesù Children's Hospital, IRCCS, Rome, Italy

[5] Radiology and Diagnostic Imaging Department, Regina Elena National Cancer Institute, IRCCS, Rome, Italy

[6] Neuro-Oncology Unit, Regina Elena National Cancer Institute, IRCCS, Rome, Italy

Correspondence
Alberto Di Napoli, Neuroradiology Unit, NESMOS Department, Sant'Andrea Hospital, La Sapienza University, Via di Grottarossa 1035, Rome 00189, Italy. Radiology Department, Castelli Romani Hospital, Via Nettunense Km 11.5, Ariccia 00040, Rome, Italy.
Email: alberto.dinapoli@uniroma1.it

[#]These authors contributed equally to this work.

Funding information
This study was supported by the grant "Progetti di Ateneo 2020" from La Sapienza University (Protocol ID: RP120172B9E252BD). Funding sources did not influence any phase of the present study.

Abstract

Background and Purpose: Glioblastoma (GBM) is an aggressive primary CNS neoplasm with poor overall survival (OS) despite standard of care. On MRI, GBM is usually characterized by an enhancing portion (CET) (surgery target) and a nonenhancing surrounding (NET). Extent of resection is a long debated issue in GBM, with recent evidence suggesting that both CET and NET should be resected in <65 years old patients, regardless of other risk factors (i.e., molecular biomarkers). Our aim was to test a radiomic model for patient survival stratification in <65 years old patients, by analyzing MRI features of NET, to aid tumor resection.

Methods: Sixty-eight <65 years old GBM patients, with extensive CET resection, were selected. Resection was evaluated by manually segmenting CET on volumetric T1-weighted MRI pre and postsurgery (within 72 h). All patients underwent the same treatment protocol including chemoradiation. NET radiomic features were extracted with a custom version of Pyradiomics. Feature selection was performed with principal component analysis (PCA) and its effect on survival tested with Cox regression model. Twelve months OS discrimination was tested by *t*-test followed by logistic regression. Statistical significance was set at $p<0.05$. The most relevant features were identified from the component matrix.

Results: Five PCA components (PC1-5) explained 90% of the variance. PC5 resulted significant in the Cox model ($p = 0.002$; exp(B) = 0.686), at *t*-test ($p = 0.002$) and logistic regression analysis ($p = 0.006$). Apparent diffusion coefficient (ADC)-based features were the most significant for patient survival stratification.

Conclusions: ADC radiomic features on NET predict survival after standard therapy and could be used to improve patient selection for more extensive surgery.

KEYWORDS
GBM, MRI, neurosurgery, radiomics, survival

INTRODUCTION

Glioblastoma (GBM) is the most common and severe primary malignant brain tumor of the adult.[1] The standard of care of newly diagnosed GBM consists of surgical resection followed by concomitant radiotherapy (RT) and chemotherapy with temozolomide (TMZ).[2] The extent of resection is mainly guided by the boundary of the contrast-enhancing portion of the tumor (CET) on T1-weighted images from MRI, and directly correlates with patient survival.[3–6] RT planning is also performed following CET borders.[7] However, the overall survival (OS) of patients with GBM remains dismal, with a median of 15–17 months.[8] GBMs are known to extend beyond the border of CET, affecting brain tissue even in distant areas.[9] MRI hyperintensity surrounding the enhancing tumor on T2 and Fluid Attenuated Inversion Recovery (FLAIR) images is a common finding in GBM, representing a combination of infiltrating tumor cells and vasogenic edema, hence it is usually referred as noncontrast enhancing tumor (NET),[10,11] whose extension has been correlated with poor prognosis.[12] After surgical resection, recurrence occurs more frequently along the resection margins where NET contains more infiltrating cells.[13] NET resection has long been debated in the literature, due to exponential risk of postsurgical deficits accompanying increasing radicality.[14,15] As a consequence, it is always difficult for neurosurgeons to decide the extent of surgical resection.[16–18] Recently, a seminal study from Molinaro et al. correlated the extent of resection (both CET and NET) in GBM with OS in one of the largest cohorts to date; their results showed that young patients (<65 years) benefit from extensive NET resection regardless of other classic outcome predictors, such as isocitrate dehydrogenase 1–2 (IDH1–2) mutation, and O^6-methylguanine-DNA methyltransferase promotor methylation status in IDH wild-type tumors.[19] The study concludes with the recommendation to pursue maximal radicality in NET resection in patients <65 years old, independently from molecular data. Since extensive resection could lead to more severe loss of functions, a detailed survival stratification is mandatory, especially in young patients.

Neuroimaging can provide useful insights for such stratification by means of noninvasive biomarkers from MRI. While conventional imaging sequences have poor accuracy in discriminating infiltrating neoplasm from vasogenic edema, with frequent overlapping features, few studies have attempted detection of viable neoplasm in NET regions by means of advanced MR techniques, such as perfusion imaging, diffusion imaging, or spectroscopy.[20–22] The rationale of such attempts lies in the correlation between MR parameters and microscopic characteristics of the brain tissue, such as cellularity for diffusion parameters[23,24] or vascularization for perfusion techniques,[25] which are typically more elevated in tumoral rather than edematous tissue. More recently, radiomics, a radiology field based on quantitative features extraction from medical images, mostly invisible to the naked eye, has shown promising results on this matter.[26] Current radiomic studies have showed the possibility of capturing NET heterogeneity, providing useful prognostic biomarkers based on conventional[27] and advanced MRI,[7] which could guide surgical resection and postoperative RT. However, most of these studies do not select patients based on the extent of resection, which is one of the main determinants of survival, creating a potential bias. Furthermore, results are often not directly applicable to the clinical practice because the studies fail to address a population of patients <65 years, which represents the main target for NET radical resection per most recent recommendations.[19]

The aim of the present study is to obtain a survival stratification of GBM patients based on radiomic features extracted from preoperative NET in both conventional (FLAIR) and advanced (diffusion weighted images [DWI] and dynamic susceptibility contrast perfusion weighted images [DSC-PWI]) MRI sequences in a selected population of young patients (<65 years) who underwent extensive CET resection of pathologically proven GBM. Our goal is to identify noninvasive MR biomarkers predictive of patient survival to help the decision of extended surgical radicality in this specific population.

METHODS

Subjects

This retrospective observational study was conducted in agreement with the Helsinki declaration and was approved by the institutional IRB (protocol number: 19 SA_2020). We selected patients with a diagnosis of GBM, who underwent preoperative MRI from March 2005 to May 2019, and underwent extensive (>80%) CET resection.[6] To evaluate survival stratification based NET only, we excluded patients with CET resection <80% since the residual tumor may significantly impact survival in this group.[6] Data were collected on a 1.5T scanner (Magnetom Sonata, Siemens, Erlangen, Germany). We enrolled patients fulfilling the following inclusion criteria: histopathological diagnosis of GBM; preoperative MRI with structural images and diffusion or perfusion techniques; postoperative MRI within 72 h from surgery with structural images; >80% CET resection as demonstrated on MRI; and availability of survival data. Exclusion criteria were motion artifacts or other causes of suboptimal images, loss of patients' information during follow-up.

All patients received postoperative focal RT plus concomitant daily TMZ, followed by adjuvant TMZ therapy, with the same treatment protocol. RT started within 4 weeks of surgery and consisted of fractionated focal irradiation at a dose of 60 Gy, delivered in 30 fractions of 2 Gy over 6 weeks. Concomitant chemotherapy consisted of TMZ in a dose of 75 mg/m^2 administered 7 days/week from the first day of RT. Adjuvant TMZ therapy began 4 weeks after the end of RT and was delivered for 5 days every 28 days, up to 12 cycles. The dose was 150 mg/m^2 for the first cycle and was increased to 200 mg/m^2 for the second one.

Patients were labeled to discriminate between long- and short-term survivors with the threshold of 12 months from diagnosis (survival > 12 or < 12 months), based on the typical median survival time of GBM patients and previous studies.[28–30]

MR image acquisition

MR examinations were acquired with a 1.5T scanner and the following protocol: axial FLAIR [repetition time [TR]/echo time [TE] 10,000/126

ms; slice thickness [ST] 4 mm, inversion time [IT] 2500 ms; flip angle [FA] 150°; matrix 512 × 512); DWI (TR/TE 3000/84 ms; ST 5 mm; FA 90°; matrix, 256 × 256) with three levels of diffusion sensitization (*b*-values 0, 500, and 1000) and relative apparent diffusion coefficient (ADC) maps; DSC-PWI during contrast injection (Gadoteric acid; dose 0.1 mmol/kg, injection rate 5 ml/s) followed by a 20-ml saline flush, based on T2*-weighted gradient-echo echo-planar sequence (TR/TE 1490/40 ms; flip angle 90°; FOV 230 × 230 mm; matrix 128 × 128, 14 sections of 5 mm thickness, 50 volumes); magnetization prepared rapid gradient-echo (MPRAGE) (TR/TE 1840/4.4 ms; ST 1 mm; IT 1100 ms; FA 15°; matrix 256 × 256) after administration of contrast. Perfusion parametric maps were obtained through a dedicated software package OleaSphere software (version 3.0, Olea Medical, La Ciotat, France). A relative cerebral blood volume (rCBV) map was generated by using an established tracer kinetic model applied to the first-pass data.[31] As previously described,[32] the dynamic curves were mathematically corrected to reduce contrast agent leakage effects.

Image processing

For every patient, MRI sequences were automatically coregistered with reference to MPRAGE using FMRIB's Linear Image Registration Tool (FLIRT) of FSL.[33] Three regions of interest (ROIs) were manually drawn on MPRAGE and FLAIR images by a neuroradiologist (L.P., with 6 years of experience in radiology) using 3D-Slicer (https://www.slicer.org). Doubtful cases were solved as for consensus with a senior neuroradiologist (A.B., with 25 years of experience in radiology). ROIs were contrast-enhancing tumor (CET), necrosis (NEC) and whole tumor including peritumoral edema (T2). The nonenhancing tumor (NET) ROI was obtained from T2, CET, and NEC ROIs as follows: T2 – (CET+NEC).

The extent of resection was evaluated by a Resection Index (RI). Briefly, pre and postcontrast volumetric images were selected from postoperative studies performed within 72 h of surgery and automatically coregistered to MPRAGE using FLIRT of FSL. CET was manually segmented on postoperative scans by a neuroradiologist (A.D.N. with 6 years of experience in radiology) using 3D-Slicer. The enhancing tumor was distinguished from blood products by comparison between pre and postcontrast images. Doubtful cases were solved as per consensus with a senior neuroradiologist (A.B., with 25 years of experience in radiology). RI was calculated from the volume of preop and postop CET ROIs as follows: %[CET (preop) – CET (postop)]/CET(preop). The surgical resection was considered radical if more than 80% tumor was removed, similar to previous studies.[6,19]

Radiomic feature extraction and statistics

Based on recent findings,[34] we performed intensity nonstandardness correction on our multi-institutional data by scaling each image with respect to its mean value within specific the brain structure (i.e., NET ROI) using MATLAB R2017a environment (MATLAB 2017, version 9.2 - R2017a, Natick, Massachusetts: The MathWorks Inc). We did not rescale the intensity range between 0 and 255 to prevent loss of information related to image downsampling.

Radiomic features were extracted from NET on ADC, FLAIR, rCBV images by using Pyradiomics package on Python 2.7 (http://www.radiomics.io/pyradiomics.html). These sequences were chosen based on the expected capability of discriminating between hypercellular/hyperperfused tumor and edema from previous studies.[21,22] Since patients had a different combination of MR sequences, each sequence was evaluated separately in our analysis. In particular, 14 shape features, 18 intensity features, and 75 texture features (gray level co-occurrence matrix, gray level difference method, gray level size zone, gray-level run length matrix, and neighborhood gray tone different matrix texture) were extracted from original images. Additionally, we included three fractal features: box counting 2D, box counting 3D, and differential box counting (https://www.mathworks.com/matlabcentral/fileexchange/13063-boxcount), properly adapting the code of the Pyradiomics pipeline. A total of 110 original features were obtained from the NET of each MR sequence separately.

Statistical analysis was performed with SPSS (software version 20.0, Chicago, IL, USA). To reduce the dimensionality of the features, principal component analysis (PCA) was employed. A Cox regression model was exploited to test the effect of all PCA components on survival calculated in days. Feature projections onto the principal components (PC) were evaluated to determine the most relevant features for survival. In a second analysis, a two-tail *t*-test between long and short survivors with threshold at 12 months (SURV) was applied to those PCA components having significant contribution to the Cox regression model. Logistic regression was applied to validate the survival analysis. Statistical significance was set at $p<0.05$.

RESULTS

According to our inclusion criteria, 68 adult patients (mean age = 51 years, range = 35–64 years, 24 females) were selected for this study. All subjects had confirmed diagnosis of GBM and underwent extensive CET resection (>80%) as demonstrated by postoperative scans obtained within 72 h after surgery. Mean survival was 541 days. Twenty-five patients were labeled as short survivors per the 12-month threshold (mean survival 177 days), while 43 patients were labeled as long survivors per the 12-month threshold (mean survival 844 days). Patient-MR sequence distribution was as follows: 68 patients with FLAIR images; 65 patients with ADC images; and 45 patients with rCBV images.

Five PCA components were chosen as they explained 90% of the variance. Only the PCA component number 5 (PC5) was significant in the Cox model, with $p = 0.002$ and exp(B) = 0.686 (Figure 1). The most relevant features projecting to PC5 as evaluated from component matrices are reported in Table 1. Information regarding the other PCA components is reported in Tables 2–5. Only ADC-based features resulted significant for patient survival stratification. Particularly,

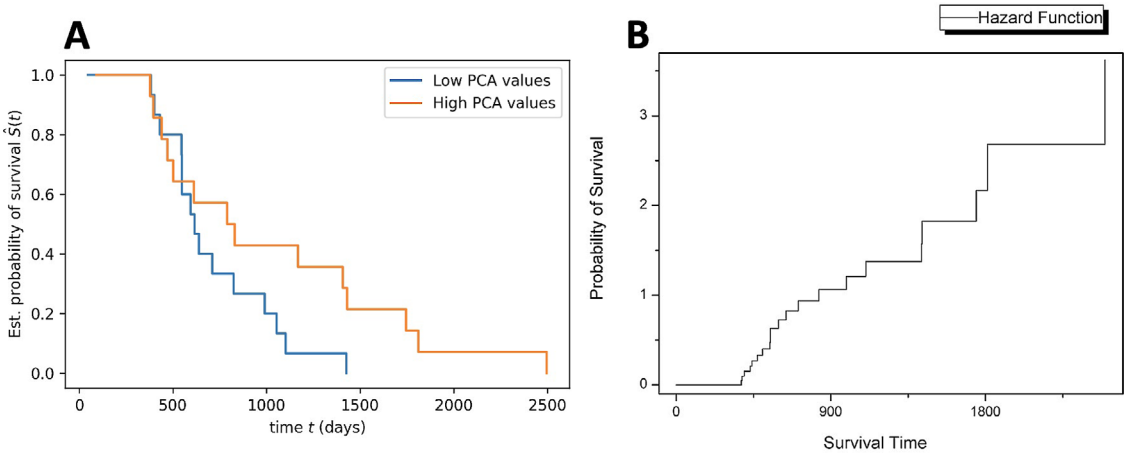

FIGURE 1 The figure describes the survival model obtained from Cox regression analysis for our patients. The image on the left (A) reports the survival function as probability of survival over time grouped by high and low principal component analysis (PCA) values (cutoff = 0.15). The image on the right (B) shows the hazard function as probability of survival over time

TABLE 1 List of the best performing features for principal component (PC) 5

PC5 ($p = 0.002$)	
Features	**Matrix values**
original_glszm_ADC_LargeAreaLowGrayLevelEmphasis	0.545
original_glszm_ADC_LargeAreaEmphasis	0.460
original_glszm_ADC_ZoneVariance	0.460
original_shape_ADC_Sphericity	0.451
original_glrlm_ADC_LongRunLowGrayLevelEmphasis	0.446
original_fractal_features_ADC_Counting3d	0.381
original_ngtdm_ADC_Busyness	0.370
original_glrlm_ADC_RunVariance	0.362
original_glrlm_ADC_LongRunEmphasis	0.319
original_firstorder_ADC_Energy	0.291

Note: The best 10 features were selected according to the absolute value of the projection's components (reported on the right). PC5 resulted significant for survival stratification ($p = 0.002$).
Abbreviation: ADC, apparent diffusion coefficient.

TABLE 2 List of the best performing features for principal component (PC) 1, selected from the component matrix

PC1 ($p = 0.181$)	
Features	**Matrix values**
original_glcm_ADC_JointEntropy	0.970
original_glcm_ADC_DifferenceEntropy	0.964
original_firstorder_ADC_Entropy	0.963
original_glcm_ADC_SumEntropy	0.958
original_firstorder_ADC_90Percentile	0.925
original_firstorder_ADC_Median	0.924
original_firstorder_ADC_MeanAbsoluteDeviation	0.923
original_firstorder_ADC_RootMeanSquared	0.921
original_firstorder_ADC_Range	0.920
original_firstorder_ADC_Mean	0.914

Note: The best 10 features were selected according to the absolute value of the projection's components (reported on the right). PC1 resulted non-significant for survival stratification ($p = 0.181$).
Abbreviation: ADC, apparent diffusion coefficient.

textural features, shape features, and fractal dimension (FD) demonstrated high relevance for PC5 (Table 1). The PC5 resulted significant in discriminating survival at 12 months as demonstrated by the two-tailed *t*-test ($p = 0.002$) (Figure 2) and logistic regression analysis ($p = 0.006$).

DISCUSSION

Our results prove that ADC-based radiomic features of the NET, obtained on presurgical MRI, are predictive of patients' survival after extensive CET resection and adjuvant chemoradiation (Figure 3).

Extension of NET has been correlated with shorter survival in both pre and postoperative setting,[35,36] as it is often the site of tumor recurrence, sometimes distant from the surgical cavity (Figure 4). For these reasons, many authors extended tumor resection beyond the borders of the CET, obtaining good correlation with increased survival.[18,37] Recently, a large cohort multicentric study by Molinaro et al. found that, in younger patients (<65 years), NET resection correlated with increased OS regardless of other survival biomarkers, such as molecular data,[19] supporting the choice of extended radicality in this specific population. Alternatively, NET removal could lead to increased postsurgical deficits,[14] as it could be hindered by increased risk of intrasurgical ischemia[38] and removal of eloquent areas (Figure 5).[39,40] The peritumoral area is, in fact, a site where brain networks, affected by tumor infiltration, tend to reorganize.[41] Identification of survival biomarkers in the NET area

TABLE 3 List of the best performing features for principal component (PC)2

PC2 ($p = 0.445$)	
Features	**Matrix values**
original_gldm_ADC_DependenceNonUniformity Normalized	0.747
original_gldm_ADC_SmallDependenceHighGray LevelEmphasis	0.634
original_glcm_ADC_ClusterProminence	0.619
original_glrlm_ADC_LongRunEmphasis	0.602
original_glrlm_ADC_RunVariance	0.596
original_glszm_ADC_SmallAreaHighGray LevelEmphasis	0.589
original_glrlm_ADC_ShortRunHighGray LevelEmphasis	0.582
original_ngtdm_ADC_Busyness	0.582
original_glcm_ADC_Autocorrelation	0.578
original_gldm_ADC_HighGrayLevelEmphasis	0.577

Note: The best 10 features were selected according to the absolute value of the projection's components (reported on the right). PC2 resulted non-significant for survival stratification ($p = 0.445$).
Abbreviation: ADC, apparent diffusion coefficient.

TABLE 4 List of the best performing features for principal component (PC) 3

PC3 ($p = 0.078$)	
Features	**Matrix values**
original_glcm_ADC_Idn	0.706
original_glcm_ADC_Idmn	0.655
original_glrlm_ADC_RunLengthNonUniformity	0.647
original_glrlm_ADC_GrayLevelNonUniformity	0.583
original_glrlm_ADC_LongRunHighGrayLevel Emphasis	0.577
original_glcm_ADC_Correlation	0.565
original_glszm_ADC_GrayLevelNonUniformity	0.560
original_gldm_ADC_LargeDependenceHighGray LevelEmphasis	0.518
original_glrlm_ADC_RunEntropy	0.497
original_glszm_ADC_ZoneEntropy	0.490

Note: The best 10 features were selected according to the absolute value of the projection's components (reported on the right). PC3 resulted non-significant for survival stratification ($p = 0.078$).
Abbreviation: ADC, apparent diffusion coefficient.

TABLE 5 List of the best performing features for principal component (PC) 4

PC4 ($p = 0.672$)	
Features	**Matrix values**
original_glcm_ADC_ClusterShade	0.718
original_firstorder_ADC_Minimum	0.589
original_gldm_ADC_DependenceNonUniformity	0.540
original_gldm_ADC_GrayLevelNonUniformity	0.511
original_gldm_ADC_Dependence NonUniformityNormalized	0.485
original_glszm_ADC_ZoneVariance	0.475
original_glszm_ADC_LargeAreaEmphasis	0.474
original_glrlm_ADC_GrayLevelNonUniformity	0.443
original_glszm_ADC_LargeAreaHighGray LevelEmphasis	0.433
original_firstorder_ADC_10Percentile	0.394

Note: The best 10 features were selected according to the absolute value of the projection's components (reported on the right). PC4 resulted non-significant for survival stratification ($p = 0.672$).
Abbreviation: ADC, apparent diffusion coefficient.

is thus advisable in order to boost patient selection for extensive resection.

Our study provides a predictive model based on radiomic features from multiparametric MRI for survival stratification in those patients who benefit from NET resection per current recommendations.[19] Other studies investigated morphological characteristics of peritumoral area to differentiate NET from vasogenic edema, mostly on T2/FLAIR images, finding a significant correlation with survival.[35,42] Some studies obtained good results in detecting viable tumor within the peritumoral region using quantitative analysis and machine-learning techniques.[22,43] A study by Choi et al. added prognostic value to GBM survival through radiomic analysis of NET on T2 images.[44] The same group developed a radiomic model using machine-learning techniques which showed better performances on survival prediction than a nonradiomic-based model.[27] Prasanna et al. found NET textural radiomic features on T1 and FLAIR images to be predictive of survival intended as less than 7 months and more than 18 months.[45] Similarly to our research, Rathore et al. analyzed multiparametric MRI to better capture NET heterogeneity; they found that recurrent GBM areas showed increased vascularity and cellularity on preoperative MRI.[7]

Our best performing features were obtained from ADC maps (Table 1), reflecting the correlation between diffusion parameters and cellularity, which may suggest cancer invasion in the peritumoral region.[24] ADC radiomic features were found predictive of GBM recurrence.[7] Also, previous research demonstrated that a peripheral habitat characterized by restricted ADC and low perfusion is more resistant to antitumoral therapies, hence could lead to shorter survival.[46] Textural features demonstrated high relevance in our analysis. These are known to express tissue heterogeneity.[47] A previous study found NET textural features to be predictive of survival on routine MRI sequences (including T2 and FLAIR).[45] In contrast, we did not find statistically significant predictive features on these sequences in our cohort. The dissimilarity could reside in a different definition of survival. Prasanna et al. opted for detecting short- (<7 months) and long-term (>18 months) survival, while we decided to evaluate prediction

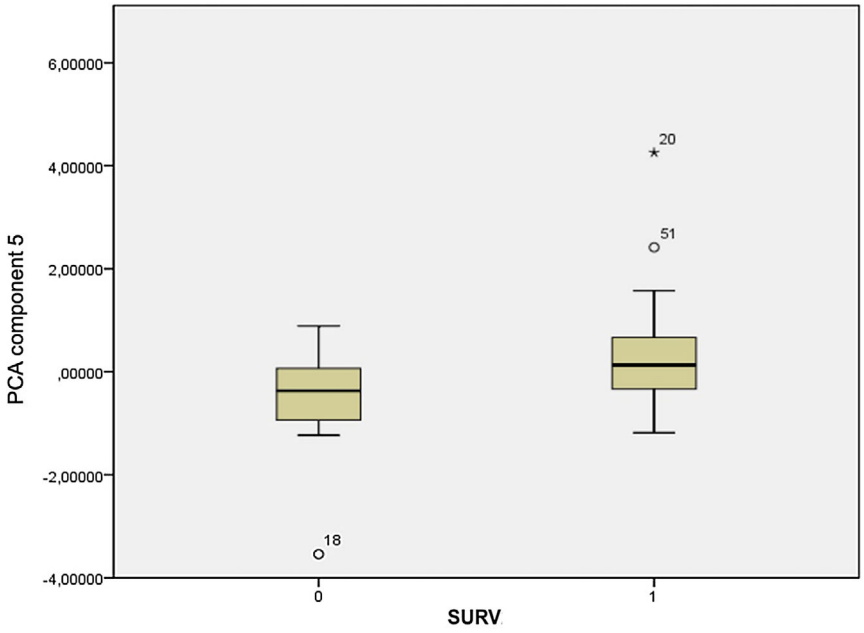

FIGURE 2 Box plots show the difference in fifth component in principal component analysis in our cohort of patients as grouped by the 12 months survival (SURV) threshold. The *t*-test analysis revealed significant difference

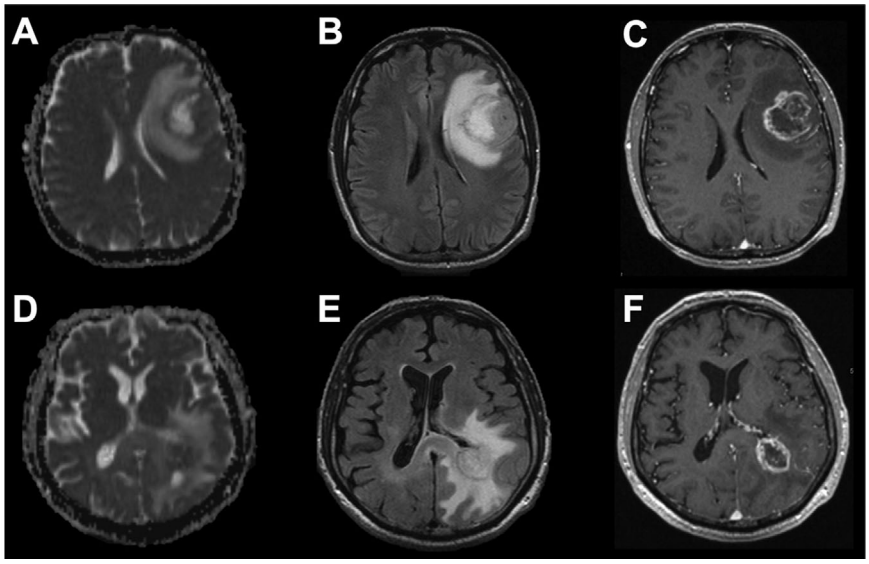

FIGURE 3 Examples of two patients evaluated in the study. Top row: MRI of a 62-year-old male with isocitrate dehydrogenase 1 (IDH1)-wild-type glioblastoma and >12 months survival. Axial apparent diffusion coefficient (ADC) (A); axial fluid attenuated inversion recovery (FLAIR) (B); and axial magnetization prepared rapid gradient echo (MPRAGE) with contrast (C). Bottom row: MRI of a 58-year-old male with IDH1-wild-type glioblastoma and <12 months survival. Axial ADC (D); axial FLAIR (E); axial MPRAGE with contrast (F)

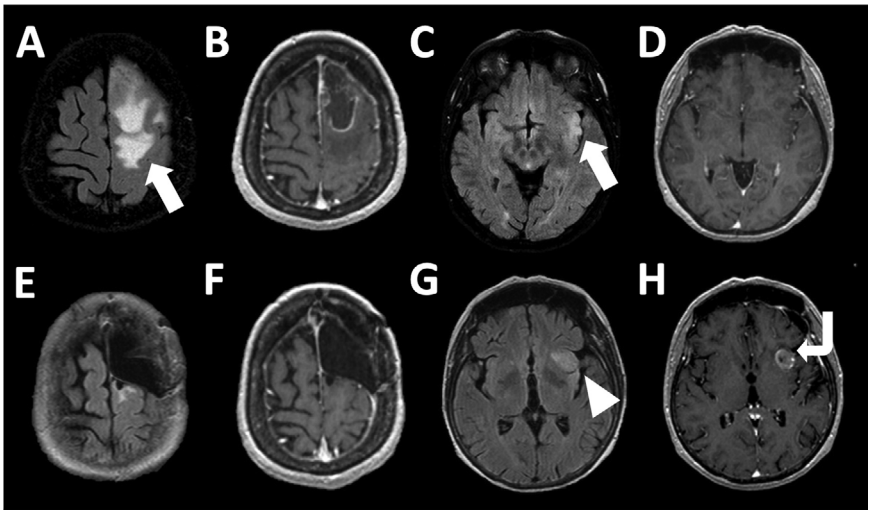

FIGURE 4 MRI of a 68-year-old male. Top row: diffuse hyperintensity on axial fluid attenuated inversion recovery (FLAIR) images (A and C) in the left superior frontal gyrus and insula (arrows) diagnosed as isocitrate dehydrogenase 1-wild-type glioblastoma; axial postcontrast images (B and D) show ring-like enhancement only in the frontal portion of the tumor. Bottom row shows a follow-up examination 6 months after surgery. Axial FLAIR images (E and G) show little hyperintensity posterior to the surgical cavity and increased hyperintensity in the insula (arrow head). Axial postcontrast images (F and H) show nodular enhancement in the insula (curved arrow) indicating tumor progression

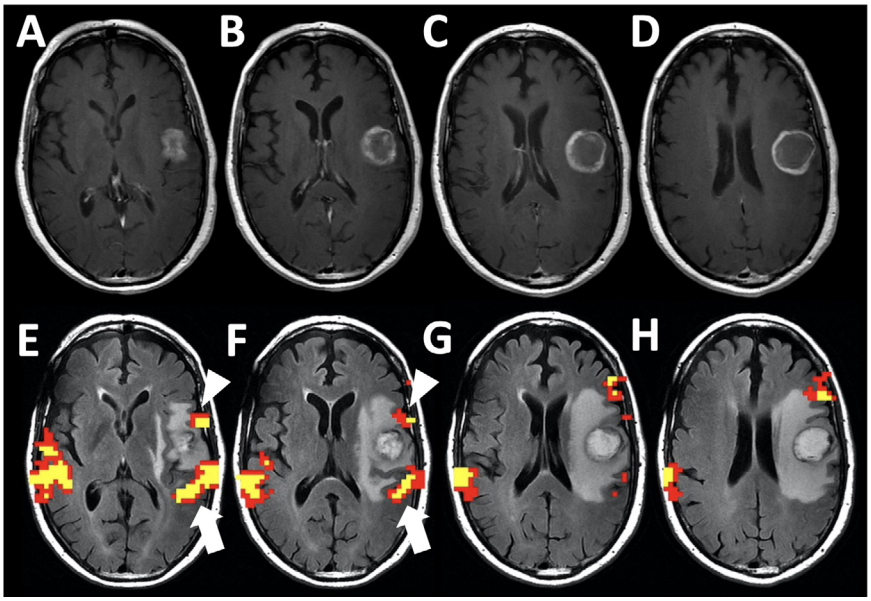

FIGURE 5 MRI of a 78-year-old right-handed male with high-grade glioma. Above: postcontrast T1-weighted MR images (A–D) show rim-enhancing tumor in the left frontal lobe invading the inferior frontal gyrus. Below: T2-weighted fluid attenuated inversion recovery images with functional MRI (fMRI) overlay displaying a semantic fluency language task. Eloquent language areas are shown as active clusters from the fMRI overlay: Broca's area is located anteriorly to the enhancing component of the tumor (arrowhead in E and F) and Wernicke's area is located posteriorly (arrow in E and F). Although the enhancing tumor does not directly infiltrate such areas, an extended resection including the nonenhancing portion (peritumoral edema) may lead to postsurgical aphasia

at 12 months, which is closer to the median survival in GBM.[8] Shape features also demonstrated high predictive performance in our analysis. In fact, such features reflect GBM irregular anisotropic growth in cluster of cells along white matter bundles.[48] In line with this and our results, shape features were already found predictive of survival in a previous study that analyzed GBM necrosis.[49] Another interesting result is the predicting value of FD. Fractal analysis is considered a reliable method to quantify tumor heterogeneity, being fractal structures that display a repeating pattern on different scales.[50] FD has been used to evaluate brain gliomas in previous studies,[51] including to differentiate GBM from lymphomas.[52] For example, FD measured on susceptibility-weighted images has been used for glioma grading.[53] On the other hand, microvascular FD showed prognostic value in GBM, including the correlation with treatment response.[54] We did not find rCBV features to be predictive of survival, differently from other studies.[55,56] As previously discussed, information from diffusion imaging, such as ADC-based features, may reflect glioma cell proliferation inside the brain tissue surrounding the enhancing tumor component. Since tumor infiltration precedes angiogenesis,[57] this may partially explain a less significant role of DSC-based information. Tumoral cell clusters in the NET region may represent proliferating habitats, which are better detected by ADC than perfusion imaging due to poor neovascularization.

Finally, following the conclusions of the large multicentric study by Molinaro et al.,[19] molecular status was not included in our analysis. However, some uncertainties still exist about the accurate molecular profiling of GBM patients, with open debate about therapeutic options.[58] Since molecular profiling of GBM is advancing at a very fast pace, the discovery of new biomarkers may lead to reconsider the relevance of molecular data for patient survival. Future studies may evaluate the correlation between radiomic data from NET regions, molecular features, and survival outcomes.

This study presents some limitations. We decided to focus only on younger patients (<65 years old) who underwent GBM extensive CET resection, due to the intent of addressing recent recommendations.[19] Our analysis required preoperative scans with multiparametric MRI and postoperative scans obtained within 72 h after surgery (see Method section). These criteria limited the possibility of using public datasets to increase our sample size. Consequently, the number of patients included in our study is somewhat narrow, yet still comparable to previous similar researches.[7,22,45,49] The retrospective nature of our study led to some imbalance in the dataset. As previously stated, not every patient had DSC perfusion imaging and this could have affected our results. Future larger, possibly multicentric, studies are needed to confirm the impact of NET-derived biomarkers on survival and validate their use in the clinical practice of patients with GBM.

To conclude, our study demonstrates that ADC radiomic features from the NET can boost survival stratification of GBM patients, possibly reflecting cell proliferation in the area surrounding the tumor mass. Textural, shape, and fractal features demonstrated high performance in our analysis, which may improve the selection of patients who benefit from more extensive surgery based on expected survival.

ACKNOWLEDGMENTS AND DISCLOSURE

The authors declare no conflicts of interest. The data presented in this study are available upon request to the corresponding author.

Open Access Funding provided by Universita degli Studi di Roma La Sapienza within the CRUI-CARE Agreement. [Correction added on 12 May 2022, after first online publication: CRUI-CARE funding statement has been added.]

ORCID

Alberto Di Napoli https://orcid.org/0000-0001-7406-7951

REFERENCES

1. Ostrom QT, Gittleman H, Stetson L, Virk SM, Barnholtz-Sloan JS. Epidemiology of gliomas. In: Raizer J, Parsa A, ed. Current Understanding and Treatment of Gliomas. Springer, Kluwer Academic Publishers; 2015:1-14.

2. Stupp R, Mason WP, Van Den Bent MJ, Weller M, Fisher B, Taphoorn MJ et al. Radiotherapy plus concomitant and adjuvant temozolomide for glioblastoma. N Engl J Med 2005;352:987-96.
3. McGirt MJ, Chaichana KL, Gathinji M, Attenello FJ Than K Olivi A, et al. Independent association of extent of resection with survival in patients with malignant brain astrocytoma: clinical article. J Neurosurg 2009;110:156-62.
4. Stummer W, Pichlmeier U, Meinel T, Wiestler OD, Zanella F, Reulen HJ. Fluorescence-guided surgery with 5-aminolevulinic acid for resection of malignant glioma: a randomised controlled multicentre phase III trial. Lancet Oncol 2006;7:392-401.
5. Stummer W, Van Den Bent MJ, Westphal M. Cytoreductive surgery of glioblastoma as the key to successful adjuvant therapies: new arguments in an old discussion. Acta Neurochir 2011;153:1211-8.
6. Sanai N, Polley MY, McDermott MW, Parsa AT, Berger MS. An extent of resection threshold for newly diagnosed glioblastomas: clinical article. J Neurosurg 2011;115:3-8.
7. Rathore S, Akbari H, Doshi J. Radiomic signature of infiltration in peritumoral edema predicts subsequent recurrence in glioblastoma: implications for personalized radiotherapy planning. J Med Imaging 2018;5:021219.
8. Molinaro AM, Taylor JW, Wiencke JK, Wrensch MR. Genetic and molecular epidemiology of adult diffuse glioma. Nat Rev Neurol 2019;15:405-17.
9. Vollmann-Zwerenz A, Leidgens V, Feliciello G, Klein CA, Hau P. Tumor cell invasion in glioblastoma. Int J Mol Sci 2020;21:1-21.
10. Barajas RF, Phillips JJ, Parvataneni R, Molinaro A, Essock-Burns E, Bourne G, et al. Regional variation in histopathologic features. Neuro Oncol 2012;14:942-54.
11. Chang EL, Akyurek S, Avalos T, Rebueno N, Spicer C, Garcia J, et al. Evaluation of peritumoral edema in the delineation of radiotherapy clinical target volumes for glioblastoma. Int J Radiat Oncol Biol Phys 2007;68:144–50.
12. Schoenegger K, Oberndorfer S, Wuschitz B, Struhal W, Hainfellner J, Prayer D, et al. Peritumoral edema on MRI at initial diagnosis: an independent prognostic factor for glioblastoma? Eur J Neurol 2009;16:874-8.
13. Ruiz-Ontañon P, Orgaz JL, Aldaz B, Elosegui-Artola A, Martino J, Berciano MT, et al. Cellular plasticity confers migratory and invasive advantages to a population of glioblastoma-initiating cells that infiltrate peritumoral tissue. Stem Cells 2013;31:1075-85.
14. Young RM, Jamshidi A, Davis G, Sherman JH. Current trends in the surgical management and treatment of adult glioblastoma. Ann Transl Med 2015;3:1-15.
15. Brown TJ, Brennan MC, Li M, Church EW, Brandmeir NJ, Rakszawski KL, et al. Association of the extent of resection with survival in glioblastoma a systematic review and meta-analysis. JAMA Oncol 2016;2:1460-9.
16. Marko NF, Weil RJ, Schroeder JL, Lang FF, Suki D, Sawaya RE. Extent of resection of glioblastoma revisited: personalized survival modeling facilitates more accurate survival prediction and supports a maximum-safe-resection approach to surgery. J Clin Oncol 2014;32:774-82.
17. Lacroix M, Abi-Said D, Fourney DR, Gokaslan ZL, Shi W, DeMonte F, et al. A multivariate analysis of 416 patients with glioblastoma multiforme: prognosis, extent of resection, and survival. J Neurosurg 2001;95:190-8.
18. Pessina F, Navarria P, Cozzi L, Ascolese AM, Simonelli M, Santoro A, et al. Maximize surgical resection beyond contrast-enhancing boundaries in newly diagnosed glioblastoma multiforme: is it useful and safe? A single institution retrospective experience. J Neuro Oncol 2017;135:129-39.
19. Molinaro AM, Hervey-Jumper S, Morshed RA, Young J, Han SJ, Chunduru P, et al. Association of maximal extent of resection of contrast-enhanced and non-contrast-enhanced tumor with survival within molecular subgroups of patients with newly diagnosed glioblastoma. JAMA Oncol 2020;6:495-503.
20. Ricci R, Bacci A, Tugnoli V, Battaglia S, Maffei M, Agati R, et al. Metabolic findings on 3T 1H-MR spectroscopy in peritumoral brain edema. AJNR Am J Neuroradiol 2007;28:1287-91.
21. Lemée JM, Clavreul A, Menei P. Intratumoral heterogeneity in glioblastoma: don't forget the peritumoral brain zone. Neuro Oncol 2015;17:1322-32.
22. Fathi Kazerooni A, Nabil M, Zeinali Zadeh M, Firouznia K, Azmoudeh-Ardalan F, Frangi AF, et al. Characterization of active and infiltrative tumorous subregions from normal tissue in brain gliomas using multiparametric MRI. J Magn Reson Imaging 2018;48:938-50.
23. Gadda D, Mazzoni LN, Pasquini L, Busoni S, Simonelli P, Giordano GP. Relationship between apparent diffusion coefficients and MR spectroscopy findings in high-grade gliomas. J Neuroimaging 2017;27:128-34.
24. la Violette PS, Mickevicius NJ, Cochran EJ, Rand SD, Connelly J, Bovi JA, et al. Precise ex vivo histological validation of heightened cellularity and diffusion-restricted necrosis in regions of dark apparent diffusion coefficient in 7 cases of high-grade glioma. Neuro Oncol 2014;16:1599-606.
25. Jain R, Griffith B, Alotaibi F, Zagzag D, Fine H, Golfinos J, et al. Glioma angiogenesis and perfusion imaging: understanding the relationship between tumor blood volume and leakiness with increasing glioma grade. AJNR Am J Neuroradiol 2015;36:2030-5.
26. Rudie JD, Rauschecker AM, Bryan RN, Davatzikos C, Mohan S. Emerging applications of artificial intelligence in neuro-oncology. Radiology 2019;00:1-12.
27. Choi Y, Ahn KJ, Nam Y, Jang J, Shin NY, Choi HS, et al. Analysis of heterogeneity of peritumoral T2 hyperintensity in patients with pretreatment glioblastoma: prognostic value of MRI-based radiomics. Eur J Radiol 2019;120:108642.
28. Yang D, Rao G, Martinez J, Veeraraghavan A, Rao A. Evaluation of tumor-derived MRI-texture features for discrimination of molecular subtypes and prediction of 12-month survival status in glioblastoma. Med Phys 2015;42:6725-35.
29. Liu Y, Xu X, Yin L, Zhang X, Li L, Lu H. Relationship between glioblastoma heterogeneity and survival time: an MR imaging texture analysis. AJNR Am J Neuroradiol 2017;38:1695-701.
30. Lee J, Jain R, Khalil K, Griffith B, Bosca R, Rao G, et al. Texture feature ratios from relative CBV maps of perfusion MRI are associated with patient survival in glioblastoma. AJNR Am J Neuroradiol 2016;37:37-43.
31. Ostergaard L, Weisskoff RM, Chesler DA, Gyldensted C, Rosen BR. High resolution measurement of cerebral blood flow using intravascular tracer bolus passages. Part I: mathematical approach and statistical analysis. Magn Reson Med 1996;36:715-25.
32. Boxerman JL, Schmainda KM, Weisskoff RM. Relative cerebral blood volume maps corrected for contrast agent extravasation significantly correlate with glioma tumor grade, whereas uncorrected maps do not. AJNR Am J Neuroradiol 2006;27:859-67.
33. Jenkinson M, Bannister P, Brady M, Smith S. Improved optimization for the robust and accurate linear registration and motion correction of brain images. Neuroimage 2002;17:825-41.
34. Um H, Tixier1 F, Bermudez D, Deasy JO, Young RJ, Veeraraghavan H. Impact of image preprocessing on the scanner dependence of multi-parametric MRI radiomic features and covariate shift in multi-institutional glioblastoma datasets. Phys Med Biol 2019;64:165011.
35. Lasocki A, Gaillard F, Tacey M, Drummond K, Stuckey S. Incidence and prognostic significance of non-enhancing cortical signal abnormality in glioblastoma. J Med Imaging Radiat Oncol 2016;60:66-73.
36. Kotrotsou A, Elakkad A, Sun J, Thomas GA, Yang D, Abrol S, et al. Multicenter study finds postoperative residual non-enhancing component of glioblastoma as a new determinant of patient outcome. J Neurooncol 2018;139:125-33.
37. Li YM, Suki D, Hess K, Sawaya R. The influence of maximum safe resection of glioblastoma on survival in 1229 patients: can we do better than gross-total resection? J Neurosurg 2016;124:977-88.

38. Gempt J, Krieg SM, Hüttinger S, Buchmann N, Ryang YM, Shiban E, et al. Postoperative ischemic changes after glioma resection identified by diffusion-weighted magnetic resonance imaging and their association with intraoperative motor evoked potentials. J Neurosurg 2013;119:829-36.
39. Picart T, Herbet G, Moritz-Gasser S, Duffau H. Iterative surgical resections of diffuse glioma with awake mapping: how to deal with cortical plasticity and connectomal constraints? Clin Neurosurg 2019;85: 105-16.
40. Li Q, del Ferraro G, Pasquini L, Peck KK, Makse HA, Holodny AI. Core language brain network for fMRI language task used in clinical applications. Netw Neurosci 2020;4:134-54.
41. Desmurget M, Bonnetblanc F, Duffau H. Contrasting acute and slow-growing lesions: a new door to brain plasticity. Brain 2007;130: 898-914.
42. Pope WB, Sayre J, Perlina A, Villablanca JP, Mischel PS, Cloughesy TF. MR imaging correlates of survival in patients with high-grade gliomas. AJNR Am J Neuroradiol 2005;26:2466-74.
43. Blystad I, Marcel Warntjes JB, Smedby O, Lundberg P, Larsson EM, Tisell A. Quantitative MRI for analysis of peritumoral edema in malignant gliomas. PLoS One 2017;12:1-12.
44. Choi Y, Ahn KJ, Nam Y, Jang J, Shin NY, Choi HS, et al. Analysis of peritumoral hyperintensity on pre-operative T2-weighted MR images in glioblastoma: additive prognostic value of Minkowski functionals. PLoS One 2019;14:1-13.
45. Prasanna P, Patel J, Partovi S, Madabhushi A, Tiwari P. Radiomic features from the peritumoral brain parenchyma on treatment-naïve multi-parametric MR imaging predict long versus short-term survival in glioblastoma multiforme: preliminary findings. Eur Radiol 2017;27:4188-97.
46. Li C, Yan JL, Torheim T, McLean MA, Boonzaier NR, Zou J, et al. Low perfusion compartments in glioblastoma quantified by advanced magnetic resonance imaging and correlated with patient survival. Radiother Oncol 2019;134:17-24.
47. Molina D, Pérez-Beteta J, Luque B, Arregui E Calvo M Borrás JM, et al. Tumour heterogeneity in glioblastoma assessed by MRI texture analysis: a potential marker of survival. Br J Radiol 2011;89: 20160242.
48. Kim Y, Lawler S, Nowicki MO, Chiocca EA, Friedman A. A mathematical model for pattern formation of glioma cells outside the tumor spheroid core. J Theor Biol 2009;260:359-71.
49. Chaddad A, Desrosiers C, Hassan L, Tanougast C. A quantitative study of shape descriptors from glioblastoma multiforme phenotypes for predicting survival outcome. Br J Radiol 2016;89:20160575.
50. Alic L, Niessen WJ, Veenland JF. Quantification of heterogeneity as a biomarker in tumor imaging: a systematic review. PLoS One 2014;9: 1-15.
51. Jang K, Russo C, di Ieva A. Radiomics in gliomas: clinical implications of computational modeling and fractal-based analysis. Neuroradiology 2020;62:771-90.
52. Liu S, Fan X, Zhang C, Wang Z, Li S, Wang Y, et al. MR imaging based fractal analysis for differentiating primary CNS lymphoma and glioblastoma. Eur Radiol 2019;29:1348-54.
53. di Ieva A, Göd S, Grabner G, Grizzi F, Sherif C, Matula C, et al. Three-dimensional susceptibility-weighted imaging at 7 T using fractal-based quantitative analysis to grade gliomas. Neuroradiology 2013;55: 35-40.
54. Chen C, He Z C, Shi Y, Zhou W, Zhang X, Xiao HL, et al. Microvascular fractal dimension predicts prognosis and response to chemotherapy in glioblastoma: an automatic image analysis study. Lab Invest 2018;98:924-34.
55. Romano A, Pasquini L, Di Napoli A, Tavanti F, Boellis A, Rossi Espagnet MC, et al. Prediction of survival in patients affected by glioblastoma: histogram analysis of perfusion MRI. J Neurooncol 2018;139: 455-60.
56. Pasquini L, Napolitano A, Tagliente E, Dellepiane F, Lucignani M, Vidiri A, et al. Deep learning can differentiate IDH-mutant from IDH-wild type GBM. J Pers Med 2021;11:290.
57. Das S, Marsden PA. Angiogenesis in glioblastoma multiforme. N Engl J Med 2013;369:1561-3.
58. Kamson DO, Grossman SA. The role of temozolomide in patients with newly diagnosed wild-type IDH, unmethylated MGMTp glioblastoma during the COVID-19 pandemic. JAMA Oncol 2021;7:675-6.

How to cite this article: Luca Pasquini, Alberto Di Napoli, Antonio Napolitano, Martina Lucignani, Francesco Dellepiane, Antonello Vidiri, Veronica Villani, Andrea Romano, Alessandro Bozzao. Glioblastoma radiomics to predict survival: diffusion characteristics of surrounding nonenhancing tissue to select patients for extensive resection. *J Neuroimaging*. 2021;31:1192–1200. https://doi.org/10.1111/jon.12903